

# Filterbank-Assisted Channel Estimation for Coherent Optical FBMC/OQAM System

Khaled A. Alaghbari , Heng-Siong Lim, Tawfig Eltaif , Benzhou Jin , *Member, IEEE*, and Lian Hong Lee

**Abstract**—In this paper, a new channel estimator for optical filter bank multicarrier with an offset-QAM modulation (FBMC/OQAM) system is proposed. The conventional channel estimation techniques that are based on interference approximation method (IAM) preamble with least squares (LS) approach suffers from sensitivity to intrinsic imaginary interference (IMI). Therefore, a filterbank-assisted (FB) technique is proposed to eliminate the residual interference associated with the preamble to improve the performance of optical FBMC/OQAM system. To further enhance the system performance, a thresholding block is added between the synthesis and analysis filter banks at the receiver to suppress the residual interference. Simulation findings show that the proposed channel estimator is more effective than the conventional IAM-R and IAM-C with LS based channel estimation at estimating the optical channel that includes chromatic dispersion and residual IMI.

**Index Terms**—FBMC/OQAM, channel estimation, intrinsic interference, chromatic dispersion, filter bank, DFT.

## I. INTRODUCTION

**F**ILTER bank multicarrier with offset-QAM modulation (FBMC/OQAM) is an emerging multicarrier technology that adds filter banks to the traditional orthogonal frequency division multiplexing (OFDM) while eliminating the need for cyclic prefix. Due to its high spectrum efficiency, lower side-lobes and resistance to narrow-band interference, it has recently attracted the attention of many researchers [1], [2]. In contrast to OFDM, only in the real field are FBMC subcarriers orthogonal, while in the imaginary field, orthogonality is lost [3], [4]. This results in intrinsic imaginary interference (IMI), which severely degrades system performance. Channel estimation is an integral part of standard coherent optical FBMC/OQAM receiver. Therefore, it is not surprising that designing channel estimator that is robust to IMI has become an important research area. Several channel estimation methods have been proposed in the literature

Manuscript received 3 October 2022; revised 28 November 2022; accepted 8 December 2022. Date of publication 14 December 2022; date of current version 19 December 2022. This work was supported by Multimedia University (MMU), Malaysia. (*Corresponding author: Khaled A. Alaghbari.*)

Khaled A. Alaghbari, Heng-Siong Lim, and Lian Hong Lee are with the Faculty of Engineering and Technology, Multimedia University (MMU), 75450 Bukit Beruang, Melaka, Malaysia (e-mail: khalidazizxp@yahoo.com; hslim@mmu.edu.my; lhlee@mmu.edu.my).

Tawfig Eltaif is with the Faculty of Engineering Technology and Science, Higher Colleges of Technology, 58855 Madinat Zayed, United Arab Emirates (e-mail: tefosat@ieee.org).

Benzhou Jin is with the College of Electronic and Information Engineering, Nanjing University of Aeronautics and Astronautics, Nanjing 211106, China (e-mail: jinbz@nuaa.edu.cn).

Digital Object Identifier 10.1109/JPHOT.2022.3228876

and one of the most promising solutions is the interference approximation method (IAM) [3], [4], [5]. In order to avoid IMI in FBMC/OQAM system, IAM employs a specially designed preamble structures such as IAM-real (IAM-R), IAM-complex (IAM-C) and enhanced IAM-C (E-IAM-C) methods. The IAM-C method is considered the best choice for channel estimation because it provides better performance over the OFDM in wireless communications [6], and lower peak-to-average-power ratio (PAPR) compared to E-IAM-C and interference cancellation methods (ICM) [4]. To improve the channel estimation method based on IAM, the authors in [7], [8] proposed to use interference approximation-based frequency averaging method. However, pilots are used in addition to IAM preamble which reduces spectral efficiency of the system. Frequency domain preamble aided channel estimation techniques are either least squares (LS) based or discrete Fourier transform (DFT) based. The LS based method is computationally less complex, however, DFT based method performs better compared to channel estimator incorporating LS based methods. The DFT based method has the capability to suppress the distortion caused by the interference in the estimated channel impulse response (CIR) [5]. However, it requires a mechanism between the IDFT and DFT modules to eliminate the residual interference (RI) and channel noise effects. In [5], Alaghbari et al. proposed an adaptive optimal channel energy algorithm to eliminate the RI and channel noise effects found in the channel impulse response (CIR). While in [9], He et al. proposed a clustering (i.e.,  $K$ -means) and discriminant analysis based method to automatically separate the noise inside the channel delay from the CIR of the conventional DFT-based channel estimation. In this paper, we replaced the IDFT and DFT modules of the conventional DFT-based channel estimation with built-in synthesis filter bank (SFB) and analysis filter bank (AFB) respectively, and without the need for complex mechanism to eliminate the RI and channel noise effects.

In traditional FBMC/OQAM receiver, one-tap frequency domain equalizer per subcarrier is typically employed to combat chromatic dispersion (CD). However, the FBMC/OQAM system still suffers from the IMI caused by adjacent subcarriers. Additional distortions found in the optical channel intensify the issue and result in inter-symbol interference (ISI) and inter-carrier interference (ICI). An  $N$ -tap frequency sampling equalizer is employed in [10] to effectively compensate for chromatic dispersion (CD), and in [11], [12] more advanced equalizer architectures are used to improve CD tolerance with trade-off between performance and complexity.

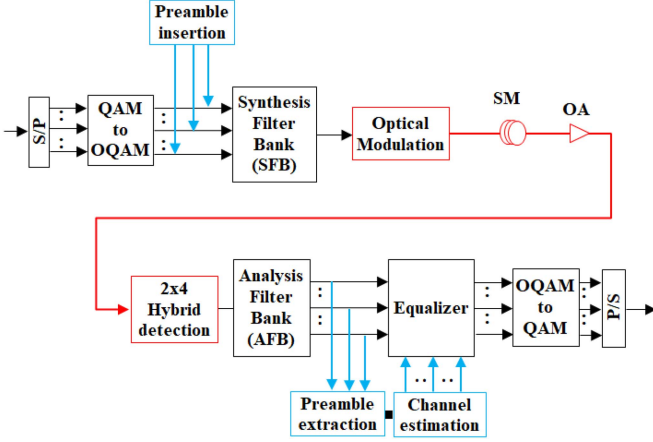


Fig. 1. Conventional coherent optical FBMC/OQAM system.

In this paper, we propose a new filterbank-assisted (FB) channel estimation technique to improve the performance of optical FBMC/OQAM system. The filterbank-assisted (FB) technique extracts the preamble and re-modulates it using the synthesis filter bank (SFB) and then filters it again with analysis filter bank (AFB) to remove the residual interference in the preamble. To further enhance the quality of CIR estimation, a threshold block is added between the SFB and AFB to suppress the distortion. The parameter of the thresholding block can be a fixed value or adaptively change based on the optical signal-to-noise ratio (OSNR). The performance of the optical FBMC/OQAM with the proposed technique is analyzed using  $N$ -tap frequency sampling equalizer under the effect of fiber chromatic dispersion and Kerr nonlinearity effect.

This paper is organized as follow: Section II presents the conventional optical FBMC/OQAM system. Section III presents the proposed filterbank-assisted channel estimator for FBMC/OQAM system. Section IV presents our new findings and discussion. Finally, conclusion is drawn in Section V.

## II. SYSTEM MODEL

Fig. 1 shows the components of a coherent optical FBMC/OQAM system. At the transmitter, data is generated, converted from serial to parallel (S/P) form and pre-processed by the QAM-to-OQAM module, which staggers the real and imaginary values of QAM symbols to form real-valued symbols  $d_{m,n}$ . The parameters  $m, n$  and  $M$  represent subcarrier index, time index and number of subcarriers respectively. To get orthogonal OQAM symbols, the symbols are multiplied by a phase factor,  $e^{j\varphi_{m,n}} = e^{j(m+n-2mn)\pi/2}$ . Hereafter, the samples are  $M/2$ -up sampled and filtered using a synthesis filter bank (SFB). In this paper, a prototype filter  $g[l]$  proposed by Bellanger [13] is used with overlapping factor  $K = 4$  and length  $L_g = KM$ . The resulted FBMC signal is given by [4]:

$$s(l) = \sum_{m=0}^{M-1} \sum_{n=0}^{N-1} d_{m,n} g_{m,n}(l) e^{j\varphi_{m,n}} \quad (1)$$

TABLE I  
TRANSMULTIPLEXER (TMUX) RESPONSE OF BELLANGER FILTER [14]

	$n-4$	$n-3$	$n-2$	$n-1$	$n_0$	$n+1$	$n+2$	$n+3$	$n+4$
$m-2$	0	$j0.0006$	0	0	0	0	0	$-j0.0006$	0
$m-1$	$j0.0054$	$-j0.0429$	$j0.1250$	$-j0.2058$	$j0.2393$	$-j0.2058$	$j0.1250$	$-j0.0429$	$j0.0054$
$m_0$	0	$j0.0668$	0	$j0.5644$	1	$-j0.5644$	0	$-j0.0668$	0
$m+1$	$-j0.0054$	$-j0.0429$	$-j0.1250$	$-j0.2058$	$-j0.2393$	$-j0.2058$	$-j0.1250$	$-j0.0429$	$-j0.0054$
$m+2$	0	$j0.0006$	0	0	0	0	0	$-j0.0006$	0

where  $g_{m,n}(l) = g(l - n\frac{M}{2} - \frac{L_g-1}{2})e^{j\frac{2\pi}{M}m(l - \frac{L_g-1}{2})}$ . After that, the FBMC/OQAM signal is modulated using an IQ optical Mach-Zehnder modulator (MZM) powered by a laser source and injected into a single mode fibre (SMF). The SMF is made up of multiple spans, each of which has an optical amplifier (OA) to compensate for the loss.

At the receiver, a  $2 \times 4$   $90^\circ$  hybrid balanced photodetectors detect and convert the received optical signal into the electrical domain. Because of orthogonality loss in FBMC/OQAM, the analysis filter bank (AFB) output at the frequency-time (FT) position  $(m_0, n_0)$ , assuming the channel frequency response (CFR) is flat and time-invariant over this subcarrier band, can be expressed as follows [4]:

$$y_{m_0, n_0} = H_{m_0} d_{m_0, n_0} + j \underbrace{\sum_{m=0}^{M-1} \sum_{n=0}^{N-1} H_m d_{m,n} g_{m_0, n_0}^{m,n}}_{i_{m_0, n_0}} + w_{m_0, n_0} \quad (2)$$

where  $H_{m_0}$  denotes the complex-valued channel frequency response,  $w_{m_0, n_0}$  defines the complex-valued additive white Gaussian noise (AWGN) and  $i_{m_0, n_0}$  represents the intrinsic imaginary interference (IMI) term affecting FT position  $(m_0, n_0)$ . If the pulse shaping filter is well localized in time and frequency so the interference is negligible outside the neighbourhood area  $\Omega_{m_0, n_0}$  of  $(m_0, n_0)$  (i.e., except  $(m_0, n_0)$  itself as shown on the shaded area of Table I), and the CIR is almost constant over this neighbourhood, (2) can be approximated as [4]:

$$y_{m_0, n_0} \cong H_{m_0} (d_{m_0, n_0} + j u_{m_0, n_0}) + w_{m_0, n_0} \quad (3)$$

where  $j u_{m_0, n_0} = \sum_{(m,n) \neq (m_0, n_0)} d_{m,n} \sum_{l=0}^{L_g-1} g_{m,n}(l) g_{m_0, n_0}^*(l)$ .

The transmultiplexer response of the Bellanger filter used in this paper is shown in Table I. It can be observed that the intrinsic interferences emanating from the symbols  $(n \pm 2)$  and  $(n \pm 3)$  are still significant in addition that caused by the nearby symbols (shaded area) [5].

The optical FBMC/OQAM signal is subjected to attenuation, chromatic dispersion (CD) and nonlinear phase noise known as Kerr effect as it propagates through the optical fiber. The CD transfer function with the absence of nonlinearity effect can be written in the Fourier domain as [15]:

$$H(\omega) = e^{j\frac{\beta_2}{2}\omega^2 z} \quad (4)$$

where  $\omega$  represents the angular frequency,  $z$  denotes the optical fiber length, and  $\beta_2$  represents second order dispersion of fiber chromatic dispersion which is also known as group velocity dispersion (GVD). Typically, dispersion is calculated using the dispersion coefficient  $D$ , which is defined as  $D = -2\pi c\beta_2/\lambda^2$ , where  $\lambda = 2\pi c/\omega$  is the wavelength of the carrier and  $c$  is the speed of light. Using the inverse DFT (IDFT) of  $H(\omega)$ , the obtained electrical discrete-time channel impulse response (CIR) can be defined as [5]:

$$h(n) = \frac{1}{M} \sum_{k=0}^{M-1} H(k) \exp\left(j2\pi \frac{nk}{M}\right), \quad 0 \leq n \leq M-1 \quad (5)$$

The received optical signal under the Kerr effect only is given by:

$$r(l) = s(l) e^{j\phi_{NL,l}} \quad (6)$$

where the nonlinear phase shift  $\phi_{NL,l}$  is given by [16]:

$$\phi_{NL,n} = \gamma L_{eff} \sum_{k=1}^{N_{span}} \left| s_n + \sum_{l=1}^k n_{l,n} \right|^2 \quad (7)$$

where  $\gamma$  represents the nonlinear coefficient,  $L_{eff}$  denotes the fiber nonlinear effective length given by  $L_{eff} = N_{span} (1 - e^{-\alpha L_{span}})/\alpha$ ,  $\alpha$  is the fiber loss,  $L_{span}$  is the fiber span length and  $n_{l,n}$  is the amplified spontaneous emission (ASE) noise of the  $l$ -th amplifier which is modelled as additive white Gaussian noise (AWGN) with zero mean and variance  $E[|n_{l,n}|^2] = 2\sigma^2$ .

The interference approximation method (IAM) is a technique that is usually used in channel estimation for FBMC/OQAM systems. The IAM preamble is inserted at the beginning of OQAM data symbols and then filtered by the SFB. The purpose of IAM is to approximate and suppress the interference by using a preamble [4]. The main idea is to make the interference emanating from the immediate neighbouring symbols (shaded area in Table I) of the preamble to nulls. Different forms of preamble have been considered in the previous studies to decrease the peak average to power ratio (PAPR) of the FBMC/OQAM signal, such as IAM-R and IAM-C which denote the real- and complex-valued preambles respectively.

The interference induced by symbols in the frequency-time locations  $(m-1, n \pm 1)$  and  $(m+1, n \pm 1)$  will be minimised by the IAM preambles. However, the Bellanger prototype filter's transmultiplexer response in the frequency-time domain is extended beyond these locations (e.g., see Table I). As a result, the intrinsic interference is not completely reduced when the least squares (LS) channel estimator is utilised for the FBMC/OQAM system, and the residual intrinsic interference becomes a source of issues.

The channel frequency response can be estimated using the least squares (LS) principle for the received preambles  $y_{m_p, n_p}$  and transmitted preambles  $d_{m_p, n_p}$  as [5]:

$$\hat{H}_{m_p, n_p}^{LS} = \frac{y_{m_p, n_p}}{d_{m_p, n_p}} = H_{m_p, n_p} + \frac{i'_{m_p, n_p} + w_{m_p, n_p}}{d_{m_p, n_p}} \quad (8)$$

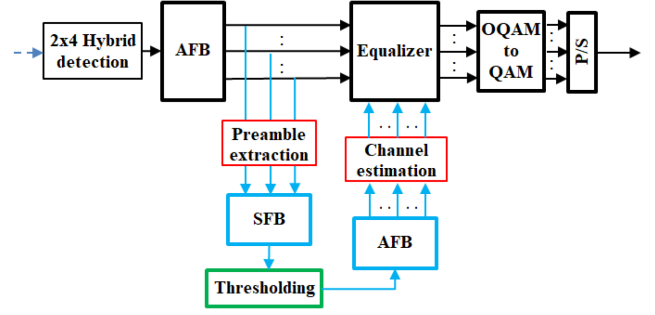


Fig. 2. FBMC/OQAM receiver based on the proposed filterbank-assisted channel estimation with threshold.

where  $i'_{m_p, n_p}$  denotes the residual intrinsic interference. The estimated channel is influenced by residual intrinsic interference and the additive Gaussian noise as shown in (8).

To eliminate the IMI and consequently improve the channel estimation of FBMC/OQAM system a method based on discrete Fourier transform (DFT) has been recently introduced in [5]. In this technique, the initial channel frequency response is first estimated from the extracted preamble using the LS approach described in (8). Then it is transformed to time domain using the inverse DFT (IDFT). A thresholding algorithm is then applied to suppress the residual intrinsic interference and the channel noise effects. Finally, the cleaned up channel impulse response is transformed back to the frequency domain using DFT.

Once the channel frequency response is estimated, the next process is to perform channel equalization to rectify the channel effects. The basic equalization technique is implemented using one-tap frequency domain equalizer per subcarrier basis; however, the one-tap equalizer does not take the ICI into account. Therefore, N-tap equalizer is suggested in [10], [11] to further eliminate the interferences, where each subcarrier is equalized with  $N_{tap}$  coefficients. The coefficient of the one-tap equalizer is obtained from the channel estimator with the number of frequency points equals to subcarriers number  $M$ . However, for N-tap equalizer, the number of frequency bins is increased by  $M(N_{tap} + 1)/2$  and obtained by interpolating the frequency response of the one-tap equalizer. Hence, the equalized signal is given by [10], [11]:

$$z_m(n) = \sum_{l_0=0}^{N_{tap}-1} c_m(l_0) \cdot y_m(n-l_0) \quad (9)$$

where  $c_m(l_0)$  is the  $N_{tap}$  equalizer coefficients obtained by interpolation.

### III. PROPOSED FILTERBANK-ASSISTED CHANNEL ESTIMATOR FOR FBMC/OQAM SYSTEM

Fig. 2 shows the proposed filterbank-assisted channel estimation technique with and without thresholding for FBMC/OQAM system. The filterbank-assisted technique is used only for the preamble (i.e., IAM-R, IAM-C, etc.). Due to the optical channel distortion and IMI, the null pilot symbols in the preamble that are initially used to prevent the middle non-zero pilot symbols from



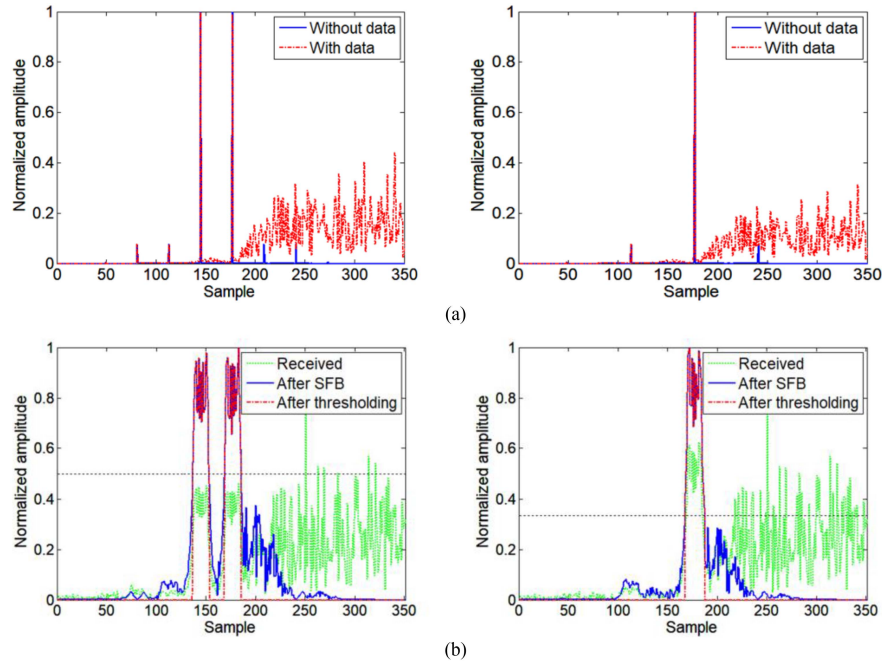


Fig. 3. Extracted IAM-R (left) and IAM-C (right) preamble samples of time-domain optical FBMC/OQAM signal at the (a) Transmitter (b) Receiver after transmission distance of 150 km.

any interference coming from previous frame and payload data are no longer purely zeros. They accumulate residual interference that can be exploited to combat the interference occurred for the non-zero pilot symbols. Therefore, the preamble extracted from the output of the AFB is first filtered by a SFB, which is a time-frequency shifted form of Bellanger prototype filter. The input of the SFB has parallel paths with one path for each subcarrier that contains the preamble samples. The results of filtering the preamble for each subcarrier are added together to form a time-domain signal  $z$ . A simple thresholding process is applied such as:

$$Threshold = \max |z| / R \quad (10)$$

where  $z$  represents the preamble signal after the SFB and the value of  $R > 1$  can have a fixed value or can be adaptively selected based on the OSNR to improve the system performance. The signal is then filtered by AFB, which is the time-reversed and complex-conjugated form of the corresponding SFB. The input of the AFB is the preamble in time-domain and the outputs are parallel signals corresponding to  $M$  subcarriers. The computational complexity of AFB or SFB using polyphase network (PPN) technique is  $4 \times (2M + M \log_2 M - 3M + 4 + 2KM)$  [12], [16]. The proposed method will increase the computation complexity by 2 times due to the usage of additional AFB and SFB.

#### IV. RESULT AND DISCUSSION

Co-simulation of the OptiSystem and Matlab softwares is used to simulate a 60 Gbps data stream with random sequences. A FBMC/4-OQAM signal is generated in Matlab using the Bellanger prototype filter [13] with an overlapping factor of  $K = 4$  and a number of subcarriers  $M = 64$ . Then by using

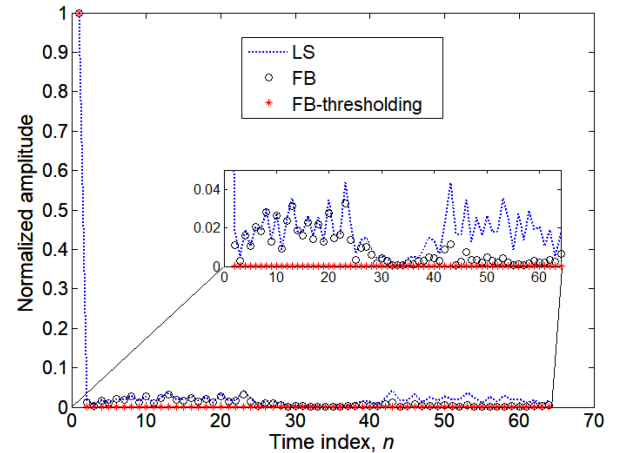


Fig. 4. Channel impulse response for conventional LS channel estimator (IAM-C) and proposed filterbank-assisted (FB) channel estimator with and without threshold for ideal case.

the OptiSystem, the signal is biased and modulated by IQ optical MZM modulator. The laser source has an input power of 5 dBm and a line-width of 1 kHz. The fiber input power is ranging between  $-20$  dBm to  $-38$  dBm in Figs. 6, 7 and 10,  $-26$  dBm in Fig. 9, and  $-14$  dBm in Figs. 3–5, measured using OptiSystem power meter. The FBMC/4-OQAM signal is then transmitted over a standard single-mode fibre (SSMF) with chromatic dispersion of 17 ps/nm/km. The optical fibre has a span of 50 km and a 10 dB optical amplifier with a noise figure of 4 dB. The OSNR is measured using OptiSystem component (WDM analyzer) after the optical amplifier. The coherent receiver is built using a  $90^\circ$  hybrid coupler and two-balanced photodiodes,

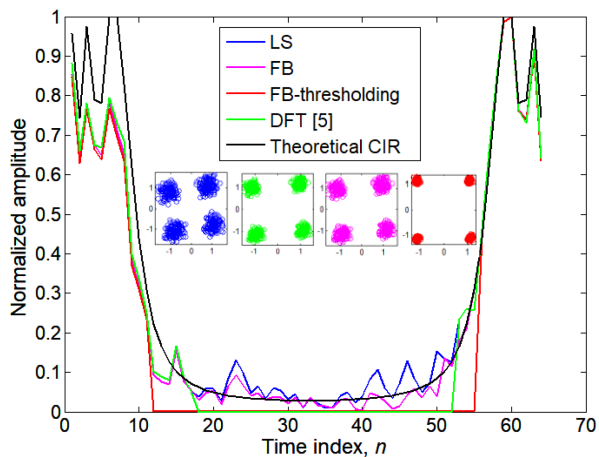


Fig. 5. Channel impulse response for conventional LS channel estimator and proposed filterbank-assisted channel estimators with and without threshold at fiber length of 150 km.

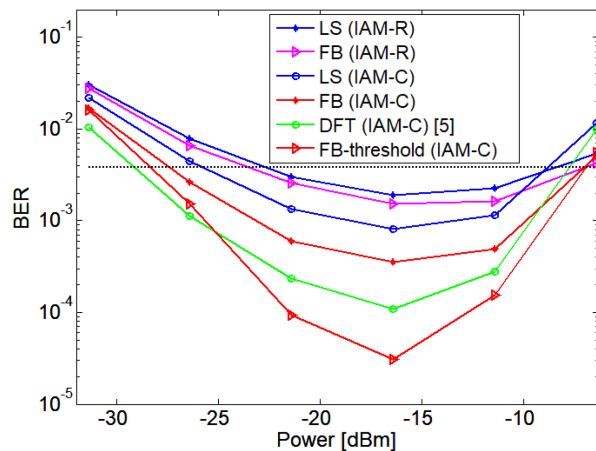


Fig. 8. BER as function of input power for conventional and proposed channel estimators at fiber length of 150 km with fiber span length of 50 km and optical amplifier of 10 dB with noise figure of 4 dB.

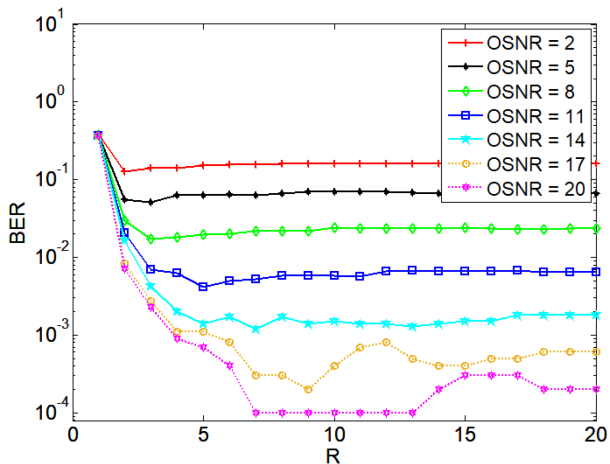


Fig. 6. BER versus  $R$  used for thresholding the proposed channel estimator.

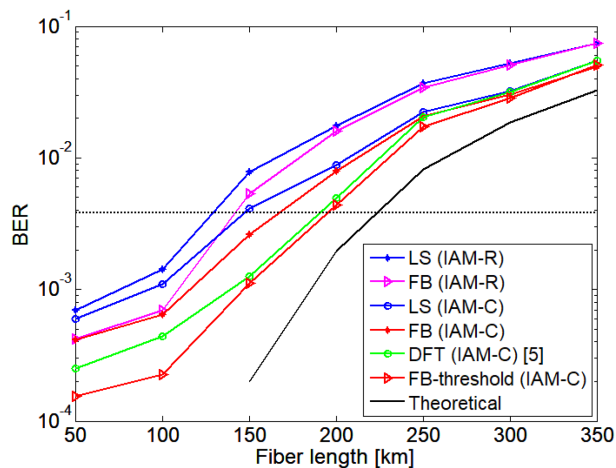


Fig. 9. BER as function of fiber length for conventional and proposed channel estimators with fiber span length of 50 km and optical amplifier of 10 dB with noise figure of 4 dB, input power  $-26.4$  dBm.

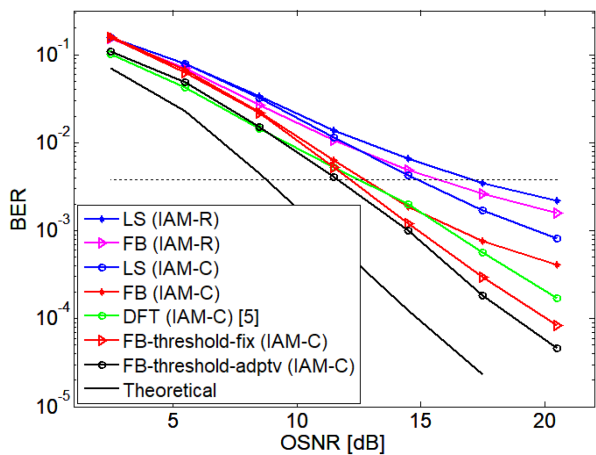


Fig. 7. BER as function of OSNR for conventional and proposed channel estimators at fiber length of 150 km with fiber span length of 50 km and optical amplifier of 10 dB with noise figure of 4 dB.

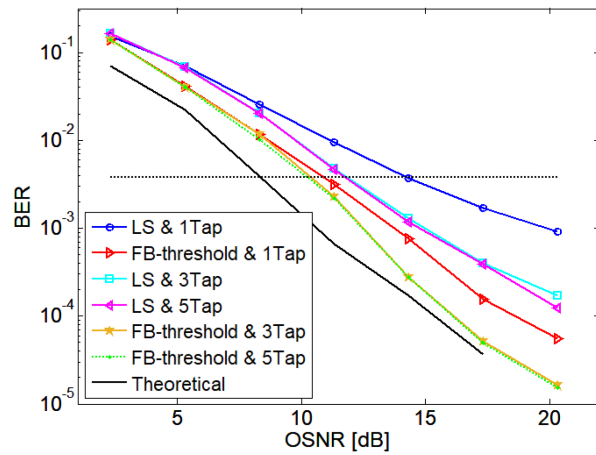


Fig. 10. BER as function of OSNR for conventional and proposed channel estimators based on IAM-C at fiber length of 150 km with  $N$ -tap sampling frequency equalizer.

with a local oscillator having same characteristics as the laser source used at the transmission side.

Since the thresholding process is performed in time domain, it is more convenient to analysis the impact of the interference based on the time-domain preamble signal. Fig. 3(a) illustrates the first samples (which contain the preamble) of the time-domain FBMC/OQAM signal at the transmitter side with data and without data using IAM-R and IAM-C preambles. The IAM-R without data has two large pulses and four small pulses, whereas IAM-C has one large pulse and two small pulses. When the data is included in the FBMC/OQAM signal the small pulses on the right-hand side overlapped with the data symbols, but the large pulses are still visible and contains higher power than the FBMC signal. At the receiver side and after transmission over 150 km optical fiber, we plotted in Fig. 3(b) the first samples of received optical FBMC/OQAM signal (in green color) that contains the preamble and the data which have been distorted by the fiber. It can be observed the pulses have been spread in time due to chromatic dispersion effect. After applying the AFB, we extracted the preamble and applied the SFB, and the result is shown in blue color. It can be observed that small amount of distortion still exists on both sides of the pulse due to residual interference caused by the optical channel and the data symbols. For channel estimation, we only interested in the preamble pulses, hence a thresholding process is applied (refer to the dotted lines) to eliminate the distortion that exceeds certain limit and improve the system performance (to be discussed next).

In Fig. 4, we plotted the channel impulse response (CIR) without considering any optical channel distortion to analyse the impact of the residual interference caused by data symbols on channel estimations. As shown in the figure, when the LS based channel estimator is used, the quality of estimated CIR is severely affected by residual interference caused by adjacent subcarriers and symbols data beyond the shaded area shown in Table I. Even though the residual interference is small, it will get more serious in the presence of the optical channel or any other source of distortion as will be discussed later. The synthesis-analysis filter bank can reduce this interference to some extent. With thresholding, the proposed filter-bank based channel estimation technique can completely eliminate the residual interference and improve the estimated CIR quality.

Fig. 5 depicts the channel impulse response (CIR) for a 30G-baud optical FBMC/OQAM system at 150 km under the effect of chromatic dispersion. The theoretical CIR is obtained using (5). The IAM-C preamble is used to generate the channel estimation shown in Fig. 5. The LS-based channel estimator cannot eliminate the effects observed in the middle of CIR due to residual intrinsic interference and optical channel effects. The FB-assisted channel estimator can reduce a small part of the distortion, as the channel estimates still fluctuates above the zero in the central section of CIR, however, it outperforms the LS-based channel estimator. The DFT-based channel estimator manages to suppress the distortion (the green line reaches zero in the central section of CIR). The FB-assisted channel estimator performs as good as the DFT-based method and completely suppressing the central section of CIR to zero by applying simple thresholding block. The eliminated taps are essentially due to the residual interference and channel effects. As shown

in the constellation diagram for each method, removing residual interference improves system performance. The constellation diagram for FB-assisted channel estimation with threshold method (in red colour) shows the cleanest constellation, while the LS based method (in blue colour) shows the worst constellation. It is worth to mention that the conventional DFT-based technique requires a mechanism between the IDFT and DFT modules to eliminate the residual distortion as in [5], [9], else its performance will be similar to LS estimator. However, the proposed FB-assisted technique still can eliminate part of the distortion without thresholding or complex mechanism.

The threshold value is optimized for the proposed channel estimator at different OSNR values, where  $R$  represents the dominator value given in (10). Fig. 6 shows that there is an optimum (minimum) value that results in good BER performance, for example, for low OSNR the  $R$  value can be approximated by 3, while for moderate OSNR it can be approximated as 5, and for high OSNR (i.e., OSNR = 17 and 20 dB) it is about 9. The proposed channel estimator can be used with fixed value of  $R$  or with dynamically changed  $R$  based on the OSNR to further improve the system performance.

Fig. 7 shows an evaluation of the IAM-R, IAM-C and our proposed filterbank-assisted channel estimators with and without threshold, the channel equalizations are performed using one tap equalizer. The IAM-C based channel estimation methods are significantly outperform the IAM-R based methods. This is because IAM-C based method has higher preamble signal power compared to IAM-R [17], which leads to better CIR estimation quality. At the BER of  $3.8 \times 10^{-3}$ , the required OSNR with LS (IAM-R) and LS (IAM-C) are 16.9 dB and 14.2 dB, respectively. Enhancement of about 3 dB can be realized by the IAM-C method compared to IAM-R based method. The filterbank-assisted technique without threshold improve the IAM-R by 1dB while improve the IAM-C by 2dB. For DFT (IAM-C), improvement of about 2 dB and 0.5 dB is achieved over the LS (IAM-C) and filterbank-assisted (IAM-C) respectively. The proposed technique with fixed threshold value (FB-threshold-fix) over all the OSNR performs better than DFT (IAM-C) at high OSNR only. To further improve the performance of the proposed filterbank-assisted based channel estimator, an adaptive threshold value (FB-threshold-adptv) can be used at each OSNR to gain more flexibility to deal with the interference. The DFT and filterbank-assisted techniques performed better than the LS based methods because they have the ability to eliminate the residual intrinsic interference found at the middle of CIR.

Fig. 8 shows the BER as a function of the input power to evaluate the nonlinearity effects on the channel estimation and equalization techniques. The operating area can be divided into two parts, linear area with input power less than  $-16$  dBm, where the BER performance of FBMC/OQAM system improves with increasing the power, and nonlinear area with input power higher than  $22$  dBm, where the BER performance of the system degrades with increasing the input power due to the nonlinearity effects. The FBMC/OQAM system with LS (IAM-R) has poor performance because the effects of CD and nonlinearity are significantly accumulated, however, at high input power, the IAM-R based method outperforms IAM-C based method because the peak-to-average-power ratio of IAM-C is higher

than IAM-R based method, and therefore it gets influenced by the fiber nonlinearity significantly. The filterbank-assisted technique can be used for both IAM-R and IAM-C with LS based channel estimator to enhance their performance. In the nonlinear region, the filterbank-assisted channel estimation with threshold outperforms other methods.

Fig. 9 illustrates the impact of fiber transmission distance in the presence of CD on the BER performance of 30GBaud coherent optical FBMC/OQAM system. LS (IAM-R) method has the humblest performance, where the required fiber length to achieve BER of  $3.8 \times 10^{-3}$  is 120 km, while the LS (IAM-C) can enhance it to 150 km. The filterbank-assisted technique without threshold can improve the performance of both methods by about 20 km. The DFT based channel estimation shows better performance than filterbank-assisted technique without threshold; however, the filterbank-assisted technique with threshold outperforms all methods and can reach near 200 km at the BER of  $3.8 \times 10^{-3}$ .

In previous figures we used 1-tap channel equalizer, however, in Fig. 10 we used advanced equalizer such as  $N$ -tap sampling frequency equalizer to test the performance of FBMC/OQAM with conventional and the proposed channel estimator. The IAM-C preamble is used for all methods, and fiber length is 150 km. As shown in Fig. 10, the 3-tap and 5-tap equalizers with LS channel estimations have improved the BER performance over the LS & 1-tap equalizer. Moreover, the proposed FB-threshold channel estimation with 3-tap/5-tap equalizer provides significant improvement over the other methods and it gets closer to theoretical curve at higher OSNR value.

## V. CONCLUSION

In this paper, a new channel estimation technique for coherent optical FBMC/OQAM system has been proposed and analyzed under chromatic dispersion and fiber nonlinearity effects. A synthesis-analysis filterbank is integrated with the channel estimator and a thresholding block with a fixed or adaptive parameter to deal with residual interference. The proposed technique enhances the quality of channel impulse response by removing the unwanted taps caused by interference and channel noise. The simulation results show that the proposed filterbank-assisted channel estimation decreases the number of bit errors and achieves significant improvement in term of OSNR, input power and fiber length over the conventional channel estimators. In addition, the filterbank-assisted channel estimation with  $N$ -tap equalization is found to perform better than LS based channel estimation with 1-tap equalizer. Future works can be done to investigate the impact of frequency offset and the usage of channel coding such as turbo codes [18] to further improve the performance of the proposed scheme.

## REFERENCES

- [1] I. S. Akila, C. Elakkiya, M. M. Priya, B. Nivedha, and S. Yadhaarshini, "Performance analysis of filter bank multicarrier system for 5G networks," in *Inventive Communication and Computational Technologies* (Lecture Notes in Networks and Systems), vol. 311, G. Ranganathan, X. Fernando, and F. Shi, Eds. Berlin, Germany: Springer, 2022, pp. 393–406.
- [2] K. A. Alaghabari, H.-S. Lim, and T. Eltaif, "Robust precoder for mitigating inter-symbol and inter-carrier interferences in coherent optical FBMC/OQAM," in *IEEE Photonics Journal*, vol. 11, no. 4, pp. 1–15, Aug. 2019, Art. no. 7904815, doi: [10.1109/JPHOT.2019.2925856](https://doi.org/10.1109/JPHOT.2019.2925856).
- [3] C. L'el'e, J.-P. Javaudin, R. Legouable, A. Skrzypczak, and P. Siohan, "Channel estimation methods for preamble-based OFDM/OQAM modulations," *Eur. Trans. Telecommun.*, vol. 19, no. 7, pp. 741–750, 2007.
- [4] E. Kofidis, D. Katselis, A. Rontogiannis, and S. Theodoridis, "Preamble-based channel estimation in OFDM/OQAM systems: A review," *Signal Process.*, vol. 93, no. 7, pp. 2038–2054, 2013.
- [5] K. A. Alaghabari, H. S. Lim, and T. Eltaif, "An improved least squares channel estimation algorithm for coherent optical FBMC/OQAM system," *Opt. Commun.*, vol. 439, pp. 141–147, 2019.
- [6] C. Lele, P. Siohan, and R. Legouable, "2dB better than CP-OFDM with OFDM/OQAM for preamble-based channel estimation," in *Proc. IEEE Int. Conf. Commun.*, 2008, pp. 1302–1306.
- [7] L. Zhang, S. Xiao, M. Bi, L. Liu, and Z. Zhou, "Channel estimation algorithm for interference suppression in IMDD-OQAM-OFDM transmission systems," *Opt. Commun.*, vol. 364, pp. 129–133, 2016.
- [8] M. Bi et al., "Low overhead equalization algorithm for simultaneously estimating channel and mitigating intrinsic imaginary interference in IMDD-OQAM-OFDM system," *Opt. Commun.*, vol. 430, pp. 256–261, 2019.
- [9] Z. He, L. Zhou, Y. Yang, Y. Chen, and X. Ling, "DFT-based channel estimation refinement by clustering in FBMC-OQAM system," *J. Eng.*, vol. 2019, no. 3, pp. 652–666, 2019.
- [10] T. H. Nguyen, F. Rottenberg, S. P. Gorza, J. Louveaux, and F. Horlin, "Efficient chromatic dispersion compensation and carrier phase tracking for optical fiber FBMC/OQAM systems," *J. Lightw. Technol.*, vol. 35, no. 14, pp. 2909–2916, Jul. 2017.
- [11] F. Rottenberg, T.-H. Nguyen, S.-P. Gorza, F. Horlin, and J. Louveaux, "Advanced chromatic dispersion compensation in optical fiber FBMC-OQAM systems," *IEEE Photon. J.*, vol. 9, no. 6, pp. 1–10, Dec. 2017, Art. no. 7204710.
- [12] K. A. Alaghabari, H. S. Lim, and T. Eltaif, "Compensation of chromatic dispersion and nonlinear phase noise using iterative soft decision feedback equalizer for coherent optical FBMC/OQAM systems," *J. Lightw. Technol.*, vol. 38, no. 15, pp. 3439–3849, Aug. 2020, doi: [10.1109/JLT.2020.2981481](https://doi.org/10.1109/JLT.2020.2981481).
- [13] M. G. Bellanger, "Specification and design of a prototype filter for filter bank based multicarrier transmission," in *Proc. IEEE Int. Conf. Acoust., Speech, Signal Process.*, 2001, pp. 2417–2420, doi: [10.1109/ICASSP.2001.940488](https://doi.org/10.1109/ICASSP.2001.940488).
- [14] S. K. Shaikhah and S. Mustafa, "Nyquist filter design," *IET Commun.*, vol. 13, no. 16, pp. 2573–2579, 2019, doi: [10.1049/iet-com.2018.6132](https://doi.org/10.1049/iet-com.2018.6132).
- [15] S. J. Savory, "Digital coherent optical receivers: Algorithms and sub-systems," *IEEE J. Sel. Topics Quantum Electron.*, vol. 16, no. 5, pp. 1164–1179, Sep./Oct. 2010.
- [16] E. Ip and J. M. Kahn, "Compensation of dispersion and nonlinear impairments using digital backpropagation," *J. Lightw. Technol.*, vol. 26, no. 20, pp. 3416–3425, Oct. 15, 2008.
- [17] E. Kofidis, L. G. Baltar, X. Mestre, F. Bader, and V. Savaux, *Orthogonal Waveforms and Filter Banks for Future Communication System*. San Diego, CA, USA: Academic Press, 2017.
- [18] K. Vasudevan, "Coherent detection of turbo-coded OFDM signals transmitted through frequency selective Rayleigh fading channels with receiver diversity and increased throughput," *Wireless Pers. Commun.*, vol. 82, no. 3, pp. 1623–1642, Jun. 2015.